ADVANCEMENT OF TiO_2-BASED PHOTOCATALYST FOR PHOTODEGRADATION OF ORGANIC POLLUTANTS IN WASTEWATER

Nurul Adilah Mohd Noor
Siti Munirah Sidik
Mohamad Saufi Rosmi
Che Ku Nor Liana Che Ku Hitam
Nur Farhana Jaafar

DOI: https://doi.org/10.37178/ca-c.21.5.081

Nurul Adilah Mohd Noor, *Department of Chemistry, Faculty of Science and Mathematics, Universiti Pendidikan Sultan Idris, 35900 Tanjong Malim, Perak, Malaysia*

Siti Munirah Sidik, *Department of Chemistry, Faculty of Science and Mathematics, Universiti Pendidikan Sultan Idris, 35900 Tanjong Malim, Perak, Malaysia*
Email; smunirah@fsmt.upsi.edu.my

Mohamad Saufi Rosmi, *Department of Chemistry, Faculty of Science and Mathematics, Universiti Pendidikan Sultan Idris, 35900 Tanjong Malim, Perak, Malaysia*

Che Ku Nor Liana Che Ku Hitam, *School of Chemical and Energy Engineering, Universiti Teknologi Malaysia, 81310 Johor Bharu, Johor, Malaysia*

Nur Farhana Jaafar, *School of Chemical Sciences, Universiti Sains Malaysia, 11800 Gelugor, Penang, Malaysia*

Abstract

Photocatalytic degradation has gained attention as an environmental friendly technology as it offers mild reaction conditions for wastewater treatment. The present review mainly describes the strategies to improve the photodegradation of organic pollutants through modification of TiO_2-based photocatalyst since TiO_2 has several disadvantages, like wide band gap (E_g) (3.2 eV) and quick recombination of photogenerated charges that inhibit its full potential towards photocatalysis. Therefore, much effort to obtain excellent photocatalytic performance that includes using mesoporous materials and the addition of metal doping into the TiO_2 are highlighted to propose a mechanistic study of promising photocatalytic method. Incorporating mesoporous materials within the TiO_2 enhance the interaction of organic pollutant and photocatalyst as

it produces large surface areas that improve the photocatalytic activity. Doping with metal will suppress the recombination between electron/hole pairs produced on photon absorption as it acts as electron sinks that may improve the photocatalytic performance by the quantum yield of superoxide radicals.

Keywords: *TiO_2; Synthesis method; Mesoporous material; Metal doping; Photodegradation; Organic pollutant*

INTRODUCTION

Nowadays, water pollution has become the main problem in the world's top environmental problems. Every single day, the death of millions of people drinking polluted water increases because this polluted water leads to various infectious diseases. The cleanliness of water for agricultural, domestic and industrial use is getting worse with the rising number of industrialization and urbanization [12]. Organic effluents such as textile, paint and leather released into water are extremely difficult to be degraded or eliminated by nature which in the end can seriously affect marine systems and human well-being [74]. Therefore, removing the organic pollutants mentioned are needed in order to avoid the surroundings as well as human health being in danger.

Previously, several methods for wastewater treatment such as coagulation, physical adsorption, membrane filtration, chlorination, sedimentation, precipitation, distillation and electrolysis were developed [7,11]. However, all these methods required high preparation cost and were ineffective as the end products formed toxic metabolites or by-products [9-11]. In recent times, Advanced Oxidation Processes (AOPs) including Fenton process, UV-Photolytic technique, Photo-Fenton process, sonolysis, ozonation process as well as photocatalysis have been widely applied as active methods for the treatment of wastewater. Among these methods, photocatalysis is the most suitable method to be used since the polluted water is mitigated by using solar energy [12]. This finding is supported by [13] which stated that photocatalysis is a very useful technique as various organic toxins will be decomposed into carbon dioxide and water using very less energy and it is also an environmental friendly method. In this technique, the degradation of poisonous organic compounds and disinfectant germs can be efficiently removed by hydroxyl radical (•OH) which is a strong oxidizing agent produced through electron-hole pairs that are generated upon the irradiation of high energy light source to the photocatalyst [14]. Figure 1 illustrates the photocatalytic mechanism by semiconductor photocatalyst.

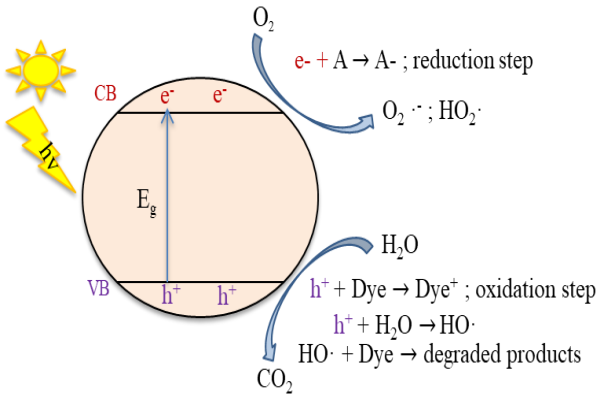

Figure 1. Schematic illustration of photocatalytic mechanism by semiconductor photocatalyst.

PHOTOCATALYSIS USING TiO_2 PHOTOCATALYST

Photocatalysis is one of the AOPs, that has been frequently used in the field of green chemistry such as wastewater treatment, exhaust gas treatment and hydrogen production in which the activity of a reaction can be enhanced with the presence of catalysts and light absorption [15]. Besides, it is also known as a promising technology due to its versatility, low-cost and promotes eco-friendly treatment for most pollutants [16]. This finding is supported by [17] which stated that, heterogeneous catalytic processes is one of the green technologies which can eliminate toxic chemicals from the environment almost completely even under mild conditions of temperature and pressure due to its broad applicability and high efficiency. The presence of light photons over a semiconductor particle (SMP) results in the formation of numerous radicals that are required for the oxidation of organic molecules in a photocatalytic process [75].

According to [19], the catalyst used was a crucial part in promoting the efficiency of photocatalytic process. Therefore, the active and selective catalysts for photodegradation of organic pollutants in wastewater are widely developed by numerous scholars. It was reported previously that semiconductor-based photocatalytic materials had gained attention as an efficient cure for cleaning up the organic effluents in wastewaters [20]. Various semiconducting metal oxide nanoparticles such as ZnO, TiO_2, WO_3, Fe_2O_3, ZnS and CdS, etc. are widely explored by researchers as photocatalysts for the removal of organic pollutants [21].

Among all, TiO_2 is known to be the most widely used semiconductor photocatalyst for the pollutants degradation because of its effectiveness and near-universal applications [22]. This finding is supported by [23, 24] which stated that TiO_2 was widely used for photocatalytic applications due to its natural abundance, stability, non-toxicity and high oxidative power of its photogenerated holes. For example, a research reported by [25] synthesized TiO_2 and titanium pillared purified clay which were prepared via sol-gel method and ion exchange reaction, respectively, for the photodegradation of selected pesticides consisted of 2,4-dichlorophenoxyacetic acid (2,4-D) and 2,4-dichlorophenoxypropionic acid (2,4-DP) as models of target pollutants. The results showed that the pesticides were efficiently degraded by these photocatalysts under UV irradiation in which TiO_2 exhibited higher photocatalytic activity than the pillared clay samples. Besides, another study reported by [26] synthesized TiO_2 nanotube (TNT) and TiO_2 nanofiber (TNF) coatings for the photodegradation of methylene blue (MB) with the irradiation of UV light. The findings showed TNF coatings exhibited more excellent photoactivity than TNT coatings. These studies has proven that TiO_2 is one of the most well-known and promising semiconducting elements for decomposing organic compounds [27].

However, TiO_2 is only active under ultraviolet radiation due to its large E_g (3.2 eV) and low separation of electron-hole pairs which has a limitation on its practical use to some extent [28-30]. This finding is supported by [31] which stated that pure TiO_2 exhibited low light absorption capacity and low charge separation adaptability that caused the limitations to occur under normal conditions. In the improvement of the photocatalytic activity of TiO_2, different modification approaches like modifying the structure, surface and morphological properties, increase the external surface area and generating the structure defects have been applied extensively [32].

The recent progress in improving the TiO_2-based photocatalyst for the elimination of pollutants in wastewater is highlighted at this point. Previous review papers mostly addressed the alteration of TiO_2-based photocatalyst via metal and non-metal doping that reduced the E_g and inhibited the recombination of electron/hole charges. For example, the review by [33] focuses on the strategies of improving TiO_2 photoactivity by doping or co-

doping of different metals and nonmetals with TiO_2 nanoparticles. Besides, another study reported by [34] focused on the improvement photoactivity of semiconductor photocatalysts via coupling between different semiconductors and metal doping technique. To date, there are minimal reviews on using mesoporous materials as a TiO_2 modification strategy. Therefore, in this review, a discussion will be presented on the further modifications of TiO_2 and TiO_2-based photocatalyst by using different synthesis methods and materials, use of mesoporous materials and metal doping for the improvement of the photocatalytic adaptability for the wastewater treatment. Hence, the findings will offer the right direction to propose a competent photocatalytic performance.

IMPROVEMENT OF TiO_2-BASED PHOTOCATALYST FOR PHOTOCATALYTIC ACTIVITY

Generally, many applications of TiO_2 depends not only on the properties of the material itself, but also its interaction with the environment [35]. Therefore, developing and improving TiO_2 to be an ideal photocatalyst should be taken into consideration in order to make this photocatalyst suitable for real-life applications.

Modification of TiO_2

Researchers have studied numerous ways to improve the photocatalytic efficiency and there has been extensive efforts in the modification of the photocatalysts. Early efforts on the modification of bare TiO_2 has been focused on the exploration of different synthesis method, different synthesis materials and the use of mesoporous structure.

TiO_2 synthesis methods

Extensive literature analysis has shown that the efficiency of photodecomposition of organic compounds by using TiO_2 is affected by the synthesis method. There are various synthesis methods like hydrothermal, sol-gel, electrochemical anodization and electrospinning have been applied to synthesis the TiO_2-based photocatalyst.

Hydrothermal method

Hydrothermal method is a heterogeneous reaction which is usually conducted in autoclaves with or without Teflon liners in the presence of aqueous solutions under a temperature or pressure that is closely monitored. The aqueous solvents are usually used under high temperature (between 100 ^oC-1000 ^oC) and pressure (between 1 atm-10 000 atm) that help to enhance the interaction of precursors during synthesis [36]. Figure 2 shows the proposed schematic illustration of the synthesizing process of TiO_2 via hydrothermal method described by [18].

Figure 2. Schematic illustration of synthesizing process of TiO_2 via hydrothermal method.

From the study, [18] was successfully synthesized TiO_2 in the form of nanotubes (TNT) that having surface area ranged from 20 m^2/g to 200 m^2/g. From the results obtained, 90% removal of MB was achieved by TNT24 within 120 min under UV irradiation which was two times better than the commercial TiO_2 nanoparticle as only 50% of MB was removed within the same duration of time. The higher degradation of MB was achieved by TNT. This is due to the higher effective surface areas and tubular structure of TNT.

Electrochemical anodization method

Another method reported to successfully synthesize TiO_2 is electrochemical anodization method. This method usually uses one from the three electrode configurations which are, a working electrode, a counter electrode and a reference electrode in an aqueous electrolyte to fabricate one dimension TiO_2 nanostructures (Figure 3).

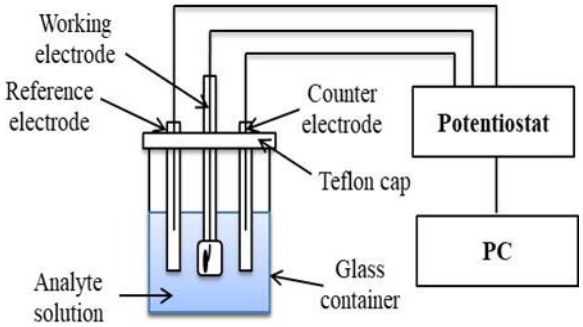

Figure 3. Schematic illustration of electrochemical anodization process with three-electrode measurement system.

In 2017, [39] was successfully synthesized a TNT film by using this method. Then, [37] managed to produce a highly ordered and oriented TNT and TiO_2 nanorod (TNR) arrays. In this study, the desired length of TNTs was obtained by varying the anodization time from 30 min to 2 h among different samples. The as-synthesized photocatalyst formed a higher amount of photocatalytic active sites and exhibited efficient adsorption of the contaminants since they had an open porous structure with higher surface area. The excellent photocatalytic activity was shown by TNT films with a length of 10 μm for both emerging contaminants caffeine (51%) and salicylic acid (50%), respectively under UV light irradiation. From the observed E_g, it also showed that the longer nanotube films exhibited narrower E_g than the shortest one, thus enhance the light absorption in the UV region.

Electrospinning method

Electrospinning method has been widely used to produce nanofibers with various functions from a variety of polymers, sol-gels, ceramics and composites due to its versatile and cost-effective technique. In this technique, high voltage was applied to give the ejection of a viscous liquid jet via a spinneret for the direct movement of charged molecules. The setup of electrospinning usually involves three major components: high voltage power supply, syringe pump and collector [37]. Figure 4 illustrates the setup of electrospinning process.

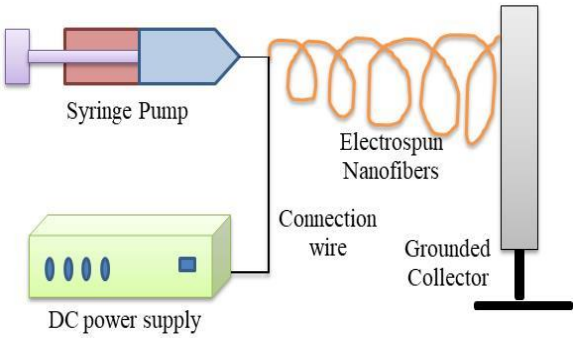

Figure 4. Schematic illustration of the setup of electrospinning process.

[38] reported on a study of synthesizing TNF using electrospinning technique. In this study, it was discovered that the synthesized photocatalyst has exhibited 19.66 m^2/g of surface area and 16.4 nm of grain size. The degradation rate of MO performed by the catalyst with UV light irradiation was used as a benchmark to measure the efficiency of photocatalytic performance. From the results obtained, the degradation of MO by pure TNF was higher than the commercial TiO_2 P25 in which 65% and 60% of MO has been decomposed, respectively. The excellent result may be attributed to the larger surface area of pure TNF compared to commercial TiO_2 P25 that has enhanced its photodegradation activity. The E_g value observed for pure TNF was 3.2 eV, and thus it performed well under UV irradiation.

Sol-gel method

Sol-gel method has also gained researchers attention to prepare nano-materials since it can be done under simple process with lower temperatures. In this method, the formation of a colloidal solution occurs as it involved hydrolysis of a titanium alkoxide and then followed by condensation. Then, a gel is obtained after applying the heat treatment (Figure 5).

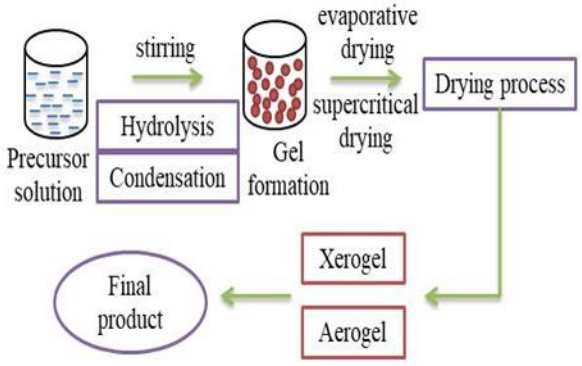

Figure 5. Schematic illustration of sol-gel process.

Adding of an acidic or basic such as hydrochloric acid (HCl) or sodium hydroxide (NaOH), respectively, can help to accelerate the reaction [37]. [40] reported about the synthesized of novel core-shell TiO_2 nanomaterials ($CSTiO_2$) via one-step smoldering combustion sol-gel method. In this study, caffeine, salicylic acid and hexavalent chromium (Cr(VI)) were degraded below UV illumination to elucidate the efficiency of the photocatalyst. From the results obtained, 65% of caffeine and salicylic acid have been

removed in 120 min and 60 min, respectively by using $CSTiO_2$ compared to pure TiO_2 that only degraded 30% of the pollutants under the same irradiation time. Meanwhile, for Cr(VI), efficient degradation has been obtained in which the pollutant was almost completely decomposed by the photocatalyst in 10 min. The excellent degradation results were obtained through the addition of urea that has enhanced TiO_2 photocatalytic activity. Besides that, the larger specific surface area of $CSTiO_2$ (175 m^2/g) compared to pure TiO_2 (48.6 m^2/g) also helped to improve the photocatalytic activity as more photoexcited electrons will be formed to inhibit the recombination of charge carriers.

TiO_2 synthesis materials

The efficient performance of photocatalysts also depends on the materials being used during the synthesizing processes. The materials properties can help to produce the photocatalysts with desired structures, morphology, crystallinity and surface area.

The study reported by [18] stated that the materials used to synthesize TNT were commercial TiO_2 P25 Degussa nanoparticles, NaOH and HCl. In this research, commercial TiO_2 was added at first into NaOH solution and then constantly stirred for 4 h. The suspension was formed during the stirring process and then it underwent hydrothermal treatment by transferring it into a Teflon-lined autoclave container, securely sealed and put in an oven at 180 ^oC. The different reaction times for hydrothermal treatment was done in order to diversify the effective surface areas of TNT. The product formed was treated with HCl solution overnight before washing using 5 L bottle tap water until the decanter water reached the pH 7. Lastly, the sample formed was filtered, dried at 60 ^oC and grounded to fine particles.

[39] synthesized TNT films by using titanium foils, Pt mesh, ethylene glycol, distilled water and ammonium fluoride (NH_4F). First of all, both of the electrodes which were free surfaces of 1.32 cm^2 from 20×20×0.125 mm titanium foils as the anodic electrode and a Pt mesh as the counter electrode were immersed into an organic electrolyte consisting of 98% vol. ethylene glycol, 2% vol. distilled water (H_2O) and 0.3% wt NH_4F. The anodization process was conducted under galvanostatic conditions in a lab-made Teflon cell by using 3.15 mA cm^{-2} with an Autolab PGSTAT-30 potentiostat (Ecochemie).

Another study by [38] synthesized pure TNF using titanium tetraisopropoxide (TTIP), polyvinylpyrrolidone (PVP), absolute ethanol and acetic acid. In this study, the viscous solution required for electrospinning was initially prepared. First, TTIP was added into the mixture of 2 mL of acetic acid, 3 mL of ethanol and 0.3 g of PVP. Then, the mixture solution was stirred for 1 h at room temperature to ensure it dissolved well. The homogeneous solution was then transferred into the syringe pump. After applying a DC voltage at 25 kV and 20 cm working distances, the solution was electrospun and a fibrous mesh was formed on the grounded collector. Lastly, the sample was calcined at 500 ^oC for 5 h by using tubular furnace.

In other study, [40] synthesized $CSTiO_2$ via one-step smoldering combustion sol-gel method. The materials to synthesize this photocatalyst consisted of titanium (IV) butoxide (TBOT), nitric acid solution (HNO_3), n-propanol and urea. First of all, 7.5 mL of TBOT was mixed together with 50 mL of HNO_3 aqueous solution and was put under vigorous stirring until it completely dissolved. After 4 h of stirring, 15 mL of n-propanol was added and turned the emulsion into transparent solution. The solution was left overnight under stirring to make it become homogenized. In this study, urea acted as the nitrogen source in which 15 g of urea added into the solution. Finally, the viscous product was obtained by gradually drying the solution at 100 ^oC and calcined for 2 h at 400 ^oC. The sample was grinded to fine powder after using the calcination process and deionized water for the purpose of eliminating the surplus organic species from the surface. The synthesized sample was

represented as $CSTiO_2$. From the reported studies, it can be concluded that the synthesis materials being used are important in order to produce the desired structure of TiO_2 photocatalyst.

Mesoporous structure

Excellent results in photodegradation of organic pollutants usually can be achieved with large surface area and high porosity of TiO_2. Recently, ordered mesoporous TiO_2 films and powders has gained researchers attention as a potential photocatalyst due to their large surface area, tunable pore diameter and nano-confined effects [41, 43]. According to [43], the large surface areas help to provide a huge number of active sites which promotes the adsorption and reaction of reactants. Besides, the transport of chemicals in the bulk of TiO_2 materials can be facilitated through produced large pore volumes which enable the accessibility of active sites. On the other hand, the use of mesoporous supports or nano-sized materials can also increase the interaction between target reactant and photocatalyst [76]. Utilization of a certain synthesis techniques have extremely affected the properties of mesoporous TiO_2 [44]. Mesoporous TiO_2 are commonly prepared via sol-gel, solvothermal, hydrothermal and microwave-assisted methods [44, 45].

Sol-gel method was first introduced by Antonelli and Ying in 1995 to synthesize mesoporous TiO_2. Preparation of mesoporous TiO_2 via sol-gel method has gained attention as the most common and versatile way since it uses low synthesis temperature and also it is easier to be carried out compared to when it is in a solid state. Besides, variety of new mesoporous TiO_2 can be prepared according to appropriate conditions. However, sol-gel process is slower in the time sense as it takes days or weeks to finish the preparation of mesoporous TiO_2. [46] reported that sol-gel technique was applied to synthesize the mesoporous hollow TiO_2 microspheres for photodegradation of 4-chlorophenol (4-CP) under UV irradiation. From the result obtained, 90% of 4-CP has been successfully degraded in 60 min. The outstanding photocatalytic performance could be attributed from inorganic hollow spheres, which is known to promote several advantages like high surface area, low compactness, mechanical and thermal stability and surface permeability. In this work, copper hydroxycarbonate ($Cu_2(OH)_2CO_3$) microsphere was used as a precursor. The mesoporous TiO_2 hollow microspheres were obtained after calcined at 400 ^oC at a heating rate of 1 ^oC/min and a dwell time of 2 h. From the characterization results, it is evident that the Brunauer-Emmet-Teller (BET) surface area, total pore volume and average pore diameter of the synthesized photocatalyst were 74.52 m^2/g, 0.23 cm^3/g and 12.37 nm, correspondingly. It also showed that, the E_g of the photocatalyst is 3.06 eV, and thus it performed well under UV irradiation.

Hydrothermal method is an environmental friendly technique and usually used for the large scale production of mesoporous TiO_2. Besides, it also does not require any post-calcination treatment, make use of aqueous solutions and facile recovery of the photocatalyst can be done after synthesizing process. This method is typically carried out in an autoclave provided with Teflon liners and a closed system under controlled temperature and pressure [71]. From a study reported [72], hydrothermal pathway was used to obtain mesoporous anatase TiO_2 in which titanium (IV) oxysulfate (TIOS), urea and sodium dodecyl sulfate (SDS) were used under aqueous medium at 180 ^oC for 24 h. From the characterization results obtained in this study, the surface area, pore volume and pore diameter of mesoporous TiO_2 were 158 m^2/g, 0.53 cm^3/g and 24.4 nm, correspondingly. In this study, the efficiency of synthesized mesoporous TiO_2 was observed through photodegradation of MB under UV and visible light. From the findings, it indicated the degradation rate of MB under UV was efficient by using the synthesized mesoporous TiO_2 in which 85-86% of MB was removed after 60 min of irradiation. However, less amount of MB was degraded by synthesized mesoporous TiO_2 under

visible light in which only 14-18% of MB was degraded because of the low photoexcitation as it has wide E_g which is 3.18 eV.

Nowadays, synthesis of mesoporous TiO_2 via microwave-assisted method has gained attention among researchers due to its several advantages such as shorter reaction times, volumetric heating ability and can start heating from interior of material body. Besides, this method is frequently applied to obtain smaller particle sizes and high purity materials [45]. [47] reported that mesoporous TiO_2 nanomaterials (MTN) had been synthesized via microwave-assisted method by varying the power densities of microwave with 0.12, 0.37 and 0.56 W/g, and represented as T1, T2 and T3, correspondingly. Figure 6 illustrates the process of synthesize MTN via microwave-assisted method.

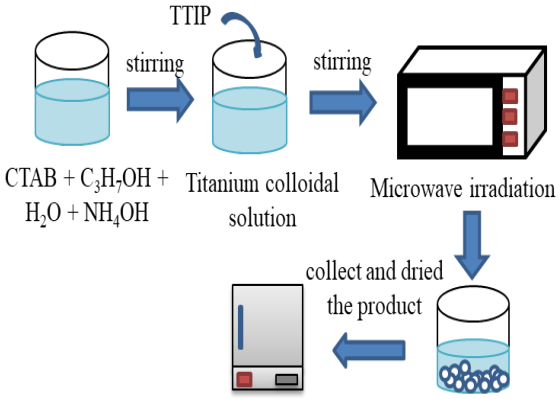

Figure 6. Schematic illustration of synthesizing MTN via microwave-assisted method.

The characterization results illustrated that MTN synthesized with higher power density was obtained larger surface area, high crystallinity, smaller particle size and low E_g. The study reported that the surface areas of T1, T2 and T3 were 152, 161 and 187 m^2/g, respectively, while the particle size was slightly decreased with 13.25, 12.24 and 11.36 nm, respectively, as the microwave power density was increased. The E_g value was also decreased for T3 compared to T1, T2 and commercial TiO_2 which exhibited 3.10 eV, 3.18 eV, 3.12 eV and 3.22 eV, respectively. Then, T1 showed the large total pore volume with 0.44 cm^3/g, followed by T2 and T3 with 0.42 and 0.36 cm^3/g, respectively. In this study, the efficiency of each synthesized MTN was examined through the degradation of 2-chlorophenol (2-CP) under irradiation of visible light and commercial TiO_2 was used as a reference photocatalyst. From the results obtained, the highest degradation was demonstrated by T3 in which 96% of 2-CP was successfully degraded under visible light. Meanwhile, the T2, T1 and commercial TiO_2 showed only 88%, 84% and 69%, respectively. The efficiency of MTN compared to commercial TiO_2 was due to the presence of oxygen vacancies (OV) and Ti^{3+} site defects (TSD) that were formed during the microwave heating. The OV and TSD helped in lowering the E_g and also operated as electron traps inhibiting the electron-hole recombination, and offered good charge carrier migration for the enhancement of photoactivity. Figure 7 illustrates the photocatalytic mechanisms of MTN via microwave-assisted method.

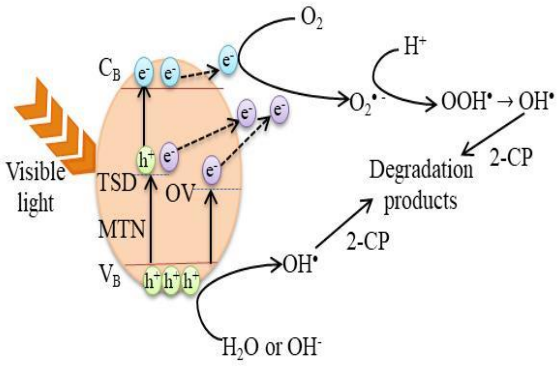

Figure 7. Schematic illustration of photocatalytic mechanism of MTN via microwave-assisted method [47].

A study from [20] highlighted the synthesized of mesoporous TiO_2 nanospheres by using solvothermal method. Solvothermal synthesis technique is often used to synthesize mesoporous materials with controlled size and high crystallinity as it can be conducted under mild reaction condition. The solvothermal pathway was nearly the same like the hydrothermal analogue apart from the solvent being used which is non-aqueous. The temperature in solvothermal reaction was practically higher than in hydrothermal method since the chosen living solvent used often has a high boiling point [44, 73]. Figure 8 shows the proposed schematic illustration of the synthesizing process of mesoporous TiO_2 through solvothermal method.

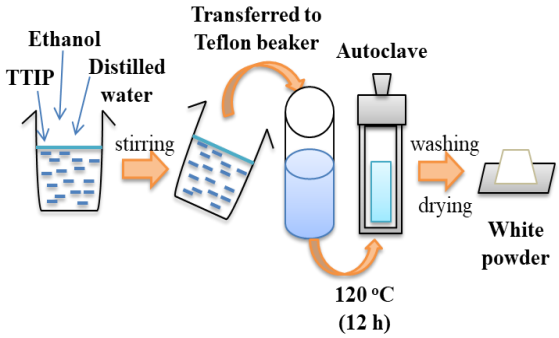

Figure 8. Schematic illustration of synthesizing mesoporous TiO_2 via solvothermal method.

The characterization results demonstrated that the surface area, pore volume and pore size of mesoporous TiO_2 nanospheres were 173 m^2/g, 0.30 cm^3/g and 3.3 nm, respectively, which confirmed that mesoporous had a well-ordered nature. The E_g value observed for mesoporous TiO_2 nanospheres was 3.16 eV. In this study, the efficiency of photocatalytic activity was determined through the degradation rate of textile dyes, which are congo red (CR), methyl orange (MO), acid orange 10 (AO10) and remazol red (RR) below solar and visible light irradiations. The results show that, the photocatalytic activity of mesoporous TiO_2 nanospheres was more active than TiO_2 P25 Degussa. It was evident when the degradation rate of CR, MO, AO10 and RR were higher by using mesoporous TiO_2 nanospheres in which 62%, 70%, 50% and 72% of degradation has been achieved

in 60 min respectively. Meanwhile, TiO_2 P25 Degussa only exhibited 50%, 62%, 42% and 68% of photodegradation, respectively. It clearly indicates that the photocatalytic reaction has been enhanced through the occurrence of anatase phase in the mesoporous TiO_2 structure by utilizing dye-sensitized mechanism that consists of continuous framework build by small particles and mesoporous nature with the large surface area and provide active sites for dye adsorption. A summary of modification of bare TiO_2 photocatalyst is shown in Table 1.

Table 1. **Summary of modification of bare TiO_2 photocatalyst**

Photocatalyst	Synthesis method	Synthesis materials	Properties			Band gap (E_g)	Pollutant	Photocatalytic performance (%)	References
			Particle size	Surface area	Pore volume				
TNT	Hydrothermal	Commercial TiO_2 P25 Degussa, HCl and NaOH	The internal diameter of TNT was in the range from 9.44 nm to 16.90 nm	Surface area of TNT formed from 20 m^2/g to 200 m^2/g	- Pore volume from 0.06 to 0.33 cm^3/g - Pore size from 4.64 to 11.61 nm	-	MB	Light source: UV light MB: 90% in 120 min	Subramaniam et al. (2017)
TNT	Electrochemical anodization	Titanium foils, Pt mesh, distilled water, ethylene glycol and NH_4F	TNT with tube lengths from 1.5 μm to 20 μm	Open porous structure with large surface area	-	Longer TNT films has narrower E_g	Caffeine and salicylic acid	Light source: UV light Caffeine: 51% in 240 min Salicylic acid: 50% in 240 min	Arfanis et al. (2017)
TNF	Electrospinning	TTIP, PVP, absolute ethanol and acetic acid	The grain size of TNF formed is 16.4 nm	Surface area of photocatalyst is 19.66 m^2/g	-	3.20 eV	MO	Light source: UV light MO: 65% in 75 min	Nasr et al. (2017)
$CSTiO_2$	Combustion sol-gel	TBOT, HNO_3, n-propanol and urea	Features an amorphous shell of approximately 1 nm thickness	Surface area of $CSTiO_2$ is 175 m^2/g	-	-	Caffeine, salicylic acid and Cr(VI)	Light source: UV light Caffeine: 65% in 120 min Salicylic acid: 65% in 60 min Cr(VI): 99% in 10 min	Arfanis et at. (2019)
Mesoporous hollow TiO_2 microspheres	Sol-gel	$Cu_2(OH)_2CO_3$, ethanol, HCl, and titanium isopropoxide (TIP)	Hollow spherical shaped particles of size 2-4 μm	Surface area of photocatalyst is 74.52 m^2/g	-Pore volume is 0.23 cm^3/g -Pore size is 12.37 nm	3.06 eV	4-CP	Light source: UV light 4-CP: 90% in 60 min	Chowdhury and Naskar (2018)
Mesoporous anatase TiO_2	Hydrothermal	TIOS, urea, SDS, deionized water and acetone	Aggregated 10-20 nm particles	Surface area of photocatalyst is 158 m^2/g	-Pore volume Is 0.53 cm^3/g -Pore diameter is 24.4 nm	3.18 eV	MB	Light source: UV light MB: 86% in 60 min	Chowdhury, Ghosh, and Naskar (2016)
MTN	Microwave-assisted	TTIP, propanol, cetyltrimethylammonium bromide (CTAB),	Particle size 11.36 to 13.25 nm	Surface area is 152 to 187 m^2/g	Pore volume from 0.36 to 0.44 cm^3/g	3.10 eV	2-CP	Light source: Visible light 2-CP:	Jaafar et al. (2015)

		distilled water and ammonium hydroxide (NH_4OH)						96% in 360 min	
Mesoporous TiO_2 nanospheres	Solvothermal	TIP, ethanol, double-distilled water and distilled water	Average size of is around ~5 nm	Surface area is 173 m^2/g	-Pore volume Is 0.30 cm^3/g -Pore size is 3.3 nm	3.16 eV	CR, MO, AO10 and RR	Light source: Solar light and visible light CR: 62% in 60 min MO: 70% in 60 min AO10: 50% in 60 min RR: 72% in 60 min	Anjugam Vandarkuzhali et al. (2018)

Doping TiO_2 with metal elements

TiO_2 is the well-known promising semiconductor photocatalyst for pollutant degradation [48] However, continuous efforts still has been put on TiO_2 modification to obtain better activity under visible light irradiation in various photocatalytic applications. One of the most common strategies is by doping TiO_2 with metal elements for better separation of photogenerated charges, and in turn will enhance the photocatalytic properties [48, 49]. This finding is supported by [50], which stated that the light absorption efficiency can be boosted by adjusting the large E_g or formation of impurity levels between the conduction band and valence band using the doping method on semiconductor photocatalysis and thus will improve the photosensitive range of a photocatalyst. Another previous study from [51-53] stated the same finding which is chemical modification by metal doping is the most widely adopted strategies that can influence the visible light absorption capability and finally will introduce the cooperative catalysts which can increase the separation between photogenerated electron and hole pairs. Figure 9 illustrates the photodegradation mechanism of doped TiO_2.

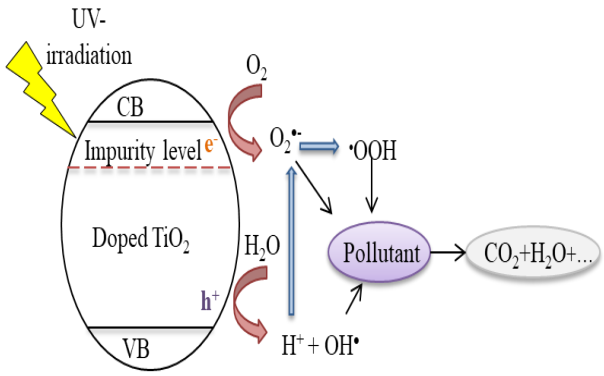

Figure 9. Schematic illustration of photodegradation mechanism of doped TiO_2.

Type of metal doping

As demonstrated in literature, the optical absorption and recombination of photogenerated carriers is significantly altered by introducing the crystal lattice of photocatalyst with electronically active secondary species [54]. Modifications of TiO_2 photocatalyst with metal doping usually include the use of noble metals (Au, Ag, Pt and Pd) and transition metals (Fe, Co and Ni) [55].

Noble metal dopant

The findings from study by [54], the photocatalytic activity of TiO_2 under visible-light irradiation was significantly developed through the effect of surface plasmon resonance (SPR) as plasmonic noble nanoparticles that has lower E_g was added in the crystal lattice of TiO_2. The SPR effect was increased due to the collective oscillations of electrons on surfaces of noble metal and formed Schottky-barrier which transferred these energetic electrons into the conduction band of the doped semiconductor. The noble metal then will act as electron acceptor, which enhances the separation of photogenerated charges [54,

56]. Figure 10 illustrates the effect of plasmonic nanoparticles towards the photocatalytic efficiency of semiconductor photocatalyst.

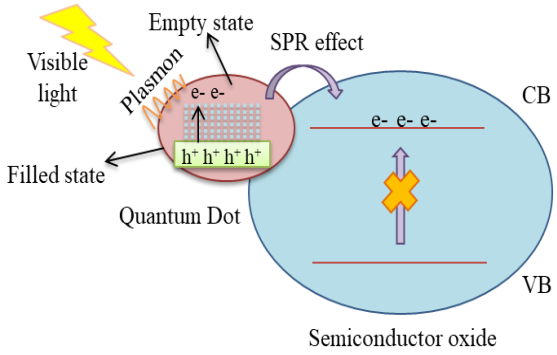

Figure 10. Plasmon nanoparticles enhanced the photocatalytic activity of semiconductor photocatalyst.

[42] studied the performance of synthesized TiO_2 nanotubes (TNT340 and TND340) and Au-modified TiO_2 nanotubes (Au/TNT340 and Au/TND340) towards MO dye under UV irradiation. The pure TiO_2 nanotubes was used as a reference to evaluate the efficiency of Au-uniform doping and Au-non-uniform doping as photocatalysts. From the result obtained, it showed that the photocatalytic activity of Au-uniformly doped TiO_2 nanotubes (Au/TNT340) and Au-non-uniformly doped TiO_2 nanotubes (Au/TND340) were higher than the TNT340 and TND340 within 25 min degradation time. This was proven when the photocatalytic efficiencies of Au/TNT340 and Au/TND340 reached up to 80.6% and 99.2%, respectively compared to TNT340 and TND340 which only exhibited 52.3% and 60%, respectively. As mentioned in literature, this is largely due to the effective separation of charge carriers as the interfaces occurred between the pure stage TiO_2 and Au-doped TiO_2 together with the contribution of 'platinum island' effect that will prevent the recombination of electron/hole pairs and thus, enhanced the photocatalysis. The observed E_g value show that the E_g of TNT340 and TND340 were smaller than the Au/TNT340 and Au/TND340 which are 3.17 eV, 3.18 eV, 3.20 eV and 3.19 eV, correspondingly. The doping of Au caused the blue shift in the absorption band edge of TNT340 and TND340. However, the E_g of Au/TND340 was smaller than the Au/TNT340 which is considered as an evidence for its highest degradation rate. These results clearly indicate that the deposition surface has been the factor of shift direction in the absorption band edge.

[58] has conducted the synthesize of Ag doped TiO_2 (Ag/TiO_2) nanoparticles via sol-gel technique. From transmission electron microscopy (TEM) micrographs, it has been confirmed that both pure TiO_2 and Ag/TiO_2 nanoparticles catalyst exhibited a non-spherical shape. The synthesized nanoparticles also showed small particle size but well crystalline in nature. The photocatalytic activity of the photocatalysts was assessed by using MB as a target pollutant to be degraded under irradiation of visible light. The findings demonstrated all doped TiO_2 photocatalysts exhibit efficient photocatalytic activity in which MB has been degraded around 72-96% during the course of irradiation compared to undoped TiO_2 which only degrade 30% of MB. The 4.0 mole% Ag-doped TiO_2 ($4\%Ag/TiO_2$) showed the highest visible-light photocatalytic activity, which can almost degrade 96% of MB within 60 min of irradiation. This result could be due to the combined effect of the dye-sensitized and synergetic action of Ag-doped TiO_2 that enhanced the

photocatalytic performance of all doped TiO_2 photocatalyst. From the observed E_g value, it clearly showed that the E_g of 4%Ag/TiO_2 was smaller than the pure TiO_2 which are 2.51 eV and 3.20 eV, respectively. These results match for its efficient result as smaller E_g can improve the photosensitive range towards visible light which enhances the photocatalytic performance. Therefore, it can be concluded that, Ag was an effective dopant to shift the optical response and enhanced the separation of charge carriers.

[59] reported the synthesize of Pt/TiO_2 nanotubes via photodeposition (PTP-1.0) and chemical reduction (PTC-1.0) methods for MO dye degradation under solar light irradiation. The TEM images of PTP-1.0 revealed the formation of bigger sized Pt particles which ranges from 4 to 10 nm with agglomeration. On the other hand, the TEM images of PTC-1.0 showed the presence of smaller Pt particles from 1.3 to 2.3 nm. It is believed that the used of capping agent in chemical reduction method help to decrease the size of Pt nanoparticles as the particle size was controlled and prevented from agglomeration to occur. As a result, PTC-1.0 exhibited higher degradation of MO dye than PTP-1.0 which were 94% and 50.5% of degradation rate, respectively, within 30 min of irradiation. The excellent performance of PTC-1.0 could be attributed to the co-existence of Pt^0, Pt^{2+}, Pt^{4+} that benefits the efficient dye decolorization instead of PTP-1.0 catalyst that consisted of only metallic Pt^0 alone. Therefore, it can be concluded that, the charge recombination will be inhibited in PTC-1.0 catalyst since the electrons formed in the conduction band will be exploited by oxidized Pt species for their reduction to Pt^0 while in the case of PTP-1.0, the presence of only Pt^0 causing recombination of charge carriers to occur since the electrons in the conduction band are not scavenged, leading to inhibit dye degradation. In this study, the incorporation of Pt loading with various oxidation state has promoted scavenger effect to occur, thus enhanced the light absorption of TiO_2 towards visible light due to the narrowing E_g.

[1] has reported the doping of noble metals (Au and Pd) with TiO_2 by incipient wet impregnation (IWI) and ultrasound-assisted impregnation (US) methods. The result of scanning electron microscopy (SEM) images for the synthesized catalysts showed the similar morphology. However, the lighter image was obtained for the sample doped with Au compared to Pd as it provides better electronic conductor. The photocatalytic activity of the prepared catalysts was assessed through the removal of 2,4 dinitrophenol (2,4 DNP) with irradiation of UV. It is evident from the data obtained that efficient photocatalytic activity was performed by the samples prepared via IWI method, and the highest 2,4 DNP degradation was exhibited by TiO_2-Pd/IWI (70%) compared to TiO_2-Au/IWI (50%) under 120 min of light irradiation. This is due to the contribution of Pd ions that enhance the formation of charge carriers and inhibit the recombination of e^-/h^+ pairs. This is in line with the E_g value of the photocatalysts, that increased in the pattern of TiO_2-Pd/IWI (2.98 eV) < TiO_2-Au/IWI (3.08 eV) < pure TiO_2 (3.20 eV).

Transition metal dopant

Eventhough noble metal dopants showed the outstanding photocatalytic activities, the rareness and high cost of noble metals making non-noble metals to be considered as more ideal co-catalysts for the large-scale application in future [2]The effect of transition metals such as cobalt (Co), iron (Fe), copper (Cu), chromium (Cr) and nickel (Ni) have been investigated by researchers to reduce the E_g, inhibit electron and hole recombination rate and apply under visible light [60]. The type and amount of transition metals are two crucial things for efficient photocatalytic activity. The separation of electrons and holes can be increased if the amount of metal dopants remain at its optimum level. However, the dopants may distort the catalyst crystallinity and act as a recombination center if they are beyond the optimum value, thus reducing the photocatalytic efficiency [61].

[4] reported the synthesize of Ni doped TiO_2 (Ni/TiO_2) catalysts via facile and rapid microwave assisted sol-gel (MW) method in which Ni contents were varied from 0.5 to 1.0 wt%, which denoted as 0.5% $Ni\text{-}TiO_2$/MW and 1.0% $Ni\text{-}TiO_2$/MW, respectively. In this study, pure TiO_2/MW and 1.0wt% Ni/TiO_2 prepared by conventional sol-gel method (1.0% $Ni\text{-}TiO_2$/CM) were used for comparative purposes. From SEM micrographs, both doped and undoped TiO_2 distributed spherical nanoparticles which consisted of agglomerates with grain sizes vary from 20-40 nm. The SEM images confirmed the improvement uniformity of particles and decreased in the particle size with the incorporation of Ni^{2+} ions. The narrowing in E_g value was also observed to the photocatalysts with Ni doping in which 1.0% $Ni\text{-}TiO_2$/MW, 0.5% $Ni\text{-}TiO_2$/MW and 1.0% $Ni\text{-}TiO_2$/CM exhibited 2.72 eV, 2.75 eV and 2.84 eV, correspondingly compared to undoped TiO_2 that perform wide E_g which is 3.08 eV. The photocatalytic activity of the prepared catalysts was assessed by bisphenol A (BPA) degradation under visible light. The findings indicated the highest degradation of BPA was obtained by 1.0% $Ni\text{-}TiO_2$/MW with 93.1% followed by 0.5% $Ni\text{-}TiO_2$/MW and pure TiO_2/MW with 83.1% and 60.1%, respectively, within 120 min. Then, when the 1.0% Ni/TiO_2 prepared by CM and MW methods was compared, only 1.0% $Ni\text{-}TiO_2$/MW showed a complete degradation in 210 min. The excellent performance of 1.0% $Ni\text{-}TiO_2$/MW catalyst could be attributed to lower E_g value, smaller crystallite size and effective separation of photogenerated charges due to the nickel incorporation. These advantages could extend the activation under visible light and thus, enhance the photocatalytic performance.

[6] reported the synthesized of Fe doped TiO_2 (Fe/TiO_2) nanoparticles via a novel and facile ultrasonic assisted hydrothermal method. From TEM analysis, it showed that both TiO_2 (bigger) and Fe dopant (smaller) particles appeared in which TiO_2 nanoparticles and Fe dopant formed in grey and dark particles, respectively. The TEM images also revealed the particles with almost spherical shaped ranging from ~10 to 20 nm. The addition of Fe dopant also has reduced the E_g value of photocatalysts, in which Fe/TiO_2 exhibited 2.90 eV which is lower than the synthesized bare TiO_2 (3.20 eV). The reduced E_g will extend the light absorption towards visible light which can advance the photocatalytic performance. The photocatalytic activity of the synthesized nanoparticles was assessed by the removal of para-nitrophenol (4-NP) and MB under visible light illumination. The result from photodegradation of aqueous solution of 4-NP with the presence of light irradiation indicated that the highest degradation was obtained with 0.05 mol% of Fe dopant, which degrade 92% of 4-NP within 300 min. This outstanding photocatalytic activity can be attributed to the maximum separation of photogenerated charge carriers that occur with the optimum value of Fe doping content. If Fe content increase more, it might lead the Fe ions to act as recombination centers for the photo-electrons and holes, thus decreasing the photocatalytic efficiency of TiO_2. Then, all the prepared catalysts were further used to degrade the textile dye, MB in order to confirm the versatility of the prepared catalysts under visible light irradiation. From the result obtained, it indicated the 0.075 mol% of Fe dopant exhibited the highest degradation, in which 93% of MB was degraded within 180 min. It was confirmed that this catalyst had high visible light response and maximum decrease in photoluminescence (PL) intensity which enhanced the separation of photo-electrons and hole-pairs.

Next, [62] reported about the synthesize of Cu-doped TiO_2-CNT nanocomposite powder using sol-gel method. In this study, the effect of incorporation of CNT and Cu doping on TiO_2 photocatalyst was observed in detail. The field emission scanning electron microscopy (FESEM) images of pure TiO_2, TiO_2-10 wt.% CNT nanocomposite (TC) and 1% Cu doped TiO_2-10 wt.% CNT nanocomposite (TCC) was observed before and after calcination. From the results obtained, the FESEM image of TCC and TC samples before calcination were similar as it showed CNT were covered by amorphous TiO_2 while pure

TiO_2 sample only showed the different sizes of spherical amorphous TiO_2 particles. However, smaller particle size and the dispersion of CNT in the microstructure was more uniformed in TCC sample compared to TC sample. The FESEM images of the three samples were then observed after calcination process. From the results, it revealed that pure TiO_2 sample formed spherical TiO_2 particles with the average particle size of 300 nm. Meanwhile, for TC sample, the surface of CNT covered by TiO_2 was observed after calcination was followed by smaller average particle size than pure TiO_2 sample of 200 nm was formed. However, more stable coating of TiO_2 on the CNT was observed in TCC sample after calcination compared to TC sample and this led to the interaction between both components of the composites to be more enhanced. The different morphology observed for TC and TCC samples was due to the addition of Cu doping in the structure of TiO_2 in which Cu^{2+} ions acted as dopants prevented the growth of TiO_2 particles during the process. The incorporation of CNT and Cu doping to TiO_2 also help in narrowing the E_g value in which TC and TCC samples exhibited 3.05 eV and 2.85 eV, respectively compared to pure TiO_2 that possesses wide E_g which is 3.20 eV. The efficiency of the as-prepared nanocomposites was confirmed via MB degradation under visible light irradiation. The findings indicated the TCC sample displayed the highest degradation of MB which was 81.5% compared to TC and pure TiO_2 samples which were 62% and 5%, respectively, within 60 min of irradiation. This excellent performance could be due to the incorporation of CNT and Cu species into TiO_2 photocatalyst. The close interaction between TiO_2 and CNT in TCC sample prolonged the electron-hole recombination since the interfacial charge transfer was enhanced. Besides, the addition of metallic Cu ions into TiO_2 also helped to inhibit the recombination of electron-hole pairs by acting as electron sink that facilitated the charge separation. The smaller particle size of TCC catalyst also contributed to high photocatalytic performance as it promoted higher surface area than freely grown TiO_2 catalyst in pure TiO_2 sample.

Another study by [63] reported about the synthesize of Cu, Fe, and Ni doped TiO_2 via sol-gel method for photodegradation of MB. FESEM analysis from this study show that the prepared photocatalysts exhibited spherical morphology. The observed E_g value showed an increment when the Cu, Fe and Ni doping was incorporated, but decreased as the amount of metal doping increased. The obtained E_g exhibited from the range of 3.22 eV to 3.42 eV, in which the smallest E_g was displayed by 9 mol% of Ni-doped TiO_2 compared to pure TiO_2. Pure TiO_2 and metal doped TiO_2 photocatalysts was used to determine the efficiency of photocatalytic activity through the degradation of MB under both UV and visible light irradiation. From the result obtained, pure TiO_2 exhibited more than 98% and 97% degradation rates of MB solution within 300 min under UV and visible light irradiation, correspondingly. It showed that the synthesized pure TiO_2 by sol gel method in this study had enhanced the photocatalytic activity compared to the commercial TiO_2 Degussa P25 which can only achieve 45% of activity under visible light within the same irradiation time [57]. The addition of transition metals (Cu, Fe and Ni) into TiO_2 had also displayed excellent photocatalytic performance under UV and visible light in which 3, 6 and 9 mol% of metal-doped TiO_2 had been studied. From the results obtained, 3 mol% of Cu and Fe-doped TiO_2 had achieved the highest photocatalytic degradation in which the percentages of MB decolorization was 97.7% and 96.9% under UV light, respectively. Meanwhile, the degradation of MB under visible light using 3 mol% of Cu and Fe-doped TiO_2 was 90% and 84.3%, respectively within 300 min of irradiation. It was proved that 3 mol% is the optimum level of Cu and Fe doping as the degradation results decreased with the increasing amount of metal concentration. However, 3 mol% of Ni-doped TiO_2 showed the highest photoactivity only under UV light in which 97.7% of MB had been decolorized. The highest degradation rate under visible light was performed by 6 mol% of Ni-doped TiO_2 in which 96.9% of MB decolorization was achieved. The further increased of these metals

into TiO_2 will reduce the photocatalytic process as it enhanced the recombination of electron and hole pairs and blocked the active sites of TiO_2 surface from light penetration.

Metal doping method

There are variety of ways to synthesize metal doped TiO_2 photocatalysts. The commonly used synthesis methods include sol-gel, wet-impregnation and hydrothermal methods. In this section, a detailed effect of different methods and conditions of TiO_2 preparation towards its physical and chemical properties will be discussed. These approaches help to imply the good control of preparation conditions which determine the effectiveness of photocatalytic performance.

The most common synthesis method for metal doping is sol-gel technique as it promotes affordable cost, high reliability, good repeatability, ease of setup process, lower temperature utilization and ease of control the physical characteristics and morphology of nanoparticles [64]. For instance, [3] has reported about the synthesize of Co doped TiO_2 with the presence of surfactant Triton X100 (TX100) or Tween 20 (T20) by using sol-gel method. In this study, phthalocyanine (Pc) derivative was used as dye sensitizer to form the photocatalyst with the presence and absence of above surfactants (Pc/Co-TiO_2). SEM images of the as-synthesized photocatalyst showed the formation of spherical like structures containing aggregated Pc molecules. From TEM image of Pc/Co-TiO_2, the average crystalline grain diameter obtained for the spherical particles were from 5-20 nm due to the agglomeration of Pc. The lighter area was assumed as the organic stage (Pc) while the darker spots on living stage proved the presence of inorganic TiO_2. In this study, the photocatalytic activity was evaluated through the degradation of MO and reduction of Cr(VI) under near visible light irradiation. The result indicated Pc/Co-TiO_2-T20 exhibited the highest photocatalytic activity, in which 60.3% of the MO and 71.3% of the Cr(VI) ions were degraded after 150 min of irradiation. The photocatalytic activity of the prepared catalysts has followed the order: Pc/Co-TiO_2-T20 > Pc/Co-TiO_2-TX100 > Pc/Co-TiO_2 > Co-TiO_2-T20 > Co-TiO_2-TX100 > Co-TiO_2. It can be concluded that, the occurrence of Tween 20 surfactant enhanced the photocatalytic performance of Co-TiO_2 by providing small crystallite size that will increase the surface area of photoactive materials. Besides, the strong absorbance of Pc added into TiO_2 structure caused the extending of catalyst's absorption edge into visible range.

Other than sol-gel method, wet-impregnation method is another option to prepare doped TiO_2. Fe doped TiO_2 (Fe/MT) nanoparticles were synthesized by [65] via wet-impregnation method. SEM images of the prepared photocatalysts demonstrated the wormhole-like mesoporous structure with large portion of intra-aggregated monodispersed nanoparticles that differs in size. As observed, the agglomeration of the nanoparticles was not influenced by the doping of different iron loadings since similar mesostructures were shown by all samples. The observed E_g value in this study showed a decrement from 3.30 eV to 2.90 eV as the Fe loading was increased, which could stabilize the separation of photogenerated charges and thus, enhance the photocatalytic activity. However, the surface area was decreased for the photocatalysts with high Fe content which possibly due to the mesopores being partially blocked in the TiO_2 support. The photocatalytic activity of degrading acid orange 7 (AO7) dye under UV-Vis and visible irradiation were significantly improved with the incorporation of iron (Fe) doping in which the dye degradation of around 99% and 54% were achieved, respectively, within 300 min of irradiation. These excellent performances can be attributed to the reducing E_g and high separation of photogenerated charges contributed by Fe^{3+} ions that were finely dispersed on the TiO_2 surface. Figure 11 shows the proposed schematic illustration of general wet-impregnation method for synthesizing a catalyst.

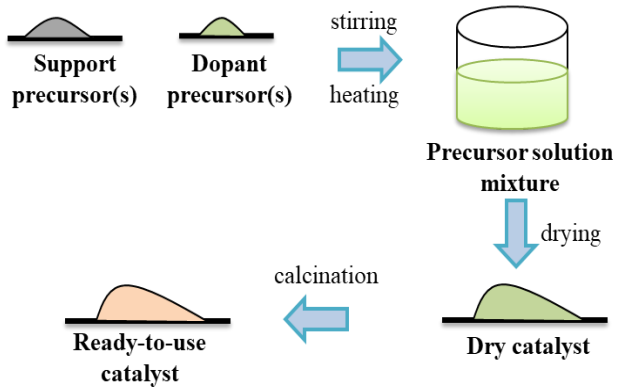

Figure 11. Schematic illustration of synthesizing catalyst via wet-impregnation method.

Hydrothermal method can also be applied in preparing doped TiO_2. The doping reaction via hydrothermal method is usually conducted in an autoclave with an exact temperature for an amount of time. The solution can be heated to a temperature above its boiling point since the reaction was conducted in an autoclave that able to withstand high pressure for the solution to achieve its vapor pressure [66]. [67] synthesized Cu doped TiO_2 (Cu/TiO_2) nanoparticles by using hydrothermal method and they observed an increment in photocatalytic activity of doped samples under visible light irradiation in which 85% of malachite green (MG) was degraded by 1.71wt.% Cu/TiO_2 within 180 min of irradiation. Meanwhile, only 53% of MG dye was degraded by using undoped TiO_2 under the same reaction conditions. It was confirmed that the expanding of Cu^{2+} content had caused decreasing in the molecule size and promote the synergistic impact that prolonged the lifetime of photogenerated e^-/h^+ pairs, hence enhanced the photocatalytic performance. The narrower E_g value was obtained as the amount of Cu doping increased in which 1.71wt.% Cu/TiO_2 exhibited the smallest E_g value, 2.34 eV compared to pure TiO_2 that formed 3.18 eV. Meanwhile, the E_g for 0.88wt.% Cu/TiO_2 and 1.52wt.% Cu/TiO_2 showed 2.72 eV and 2.48 eV, respectively. The lower E_g value of 1.71wt.% Cu/TiO_2 could be assumed as an indirect evidence of its efficient degradation rate as metal doping facilitated the separation of photogenerated carriers, thus enhanced the photocatalysis. From TEM micrograph, non-uniform shape and size of particles with agglomeration were obtained within the range of 8-10 nm. The surface area of the photocatalysts also increased with the incorporation of metal doping. A summary of doping TiO_2 with metal elements is shown in Table 2.

Table 2. **Summary of doping TiO_2 with metal elements**

Photocatalyst	Synthesis method	Light source	Experimental conditions	Surface area	Band gap (E_g)	Photocatalytic performance	References
Au/TNT	Liquid phase deposition	UV light	Catalyst : 0.5 g/L [MO] : 20 mg/L	-	Undoped TNT: 3.17 eV and 3.18 eV Au-doped: 3.19 eV and 3.20 eV	99.2% in 25 min	Zhang et al. (2017)
Ag/TiO_2	Sol-gel	Visible light	Catalyst : 1 g/L [MB] : 10 mg/L	-	Undoped TiO_2: 3.20 eV Ag-doped: 2.51 eV	96% in 60 min	Ali et al. (2018)
Pt/TiO_2	Deposition	Solar light	Catalyst : 2 g/L [MO] : 16.37 mg/L	-	The incorporation of Pt into TiO_2 has reduced the E_g	94% in 30 min	Lakshmanareddy et al. (2019)
Au/TiO_2 and Pd/TiO_2	IWI and US	UV light	Catalyst : 1 g/L [2,4 DNP] : 20 mg/L	Undoped TiO_2: 10.35 m^2/g Au/TiO_2: 10.1 m^2/g Pd/TiO_2: 11.57 m^2/g	Undoped TiO_2: 3.20 eV Au-doped: 3.08 eV Pd-doped: 2.98 eV	70% in 120 min	Sescu et al. (2021)
Ni/TiO_2	MW	Visible light	Catalyst : 1 g/L [BPA] : 10 mg/L	Undoped TiO_2: 60.3 m^2/g Ni/TiO_2: 83.5 m^2/g	Undoped TiO_2: 3.08 eV Ni-doped: 2.72 eV	93.1% in 120 min	Blanco-Vega et al. (2017)
Fe/TiO_2	Ultrasonic assisted hydrothermal	Visible light	Catalyst : 0.5 g/L [4-NP] : 10 mg/L [MB] : 10 mg/L	Undoped TiO_2: 50.21 m^2/g Fe/TiO_2: 45.04 m^2/g	Undoped TiO_2: 3.20 eV Fe-doped: 2.90 eV	4-NP: 92% in 300 min MB: 93% in180 min	Sood et al. (2015)

Cu/TiO_2-CNT	Sol-gel	Visible light	Catalyst : 0.4 g/L [MB] : 5 mg/L	Undoped TiO_2: 87.3 m^2/g TiO_2-CNT: 121.6 m^2/g Cu/TiO_2-CNT: 187.8 m^2/g	Undoped TiO_2: 3.20 eV CNT and Cu-doped: 2.85 eV	81.5% in 60 min	Shafei and Sheibani (2019)
(Cu, Fe, Ni)/TiO_2	Sol-gel	UV and Visible light	Catalyst : 1 g/L [MB] : 2.5 mg/L	Undoped TiO_2: 42.08 m^2/g Cu/TiO_2: 31.13 m^2/g Fe/TiO_2: 53.34 m^2/g Ni/TiO_2: 74.12 m^2/g	Undoped TiO_2: 3.24 eV Cu-doped: 3.26 eV Fe-doped: 3.29 eV Ni-doped: 3.22 eV	98% in 300 min	Biru et al. (2021)
Co/TiO_2 modified with Pc and surfactants (T20 and TX100)	Sol-gel	Near visible light	Catalyst : 2 g/L [MO] : 10 mg/L [Cr(VI)] : 10 mg/L	Pc/Co-TiO_2: 38.620 m^2/g Pc/Co-TiO_2-TX100: 133.937 m^2/g Pc/Co-TiO_2-T20: 151.978 m^2/g	-	MO: 60.3% in150 min Cr(VI): 71.3% in 150 min	Altin, Sokmen, and Biyiklioglu (2016)
Fe/MT	Wet-impregnation	UV and Visible light	Catalyst : 1 g/L [AO7] : 20 mg/L	Undoped TiO_2: 87 m^2/g Fe/MT: 47 m^2/g	Undoped TiO_2: 3.30 eV Fe-doped: 2.90 eV	-99% in 300 min	Rodriguez et al. (2019)
Cu/TiO_2	Hydrothermal	Visible light	Catalyst : No data [MG] : 50 mg/L	Undoped TiO_2: 139.35 m^2/g Cu/TiO_2: 197.84 m^2/g	Undoped TiO_2 3.18 eV Cu-doped: 2.34 eV	85% in 180 min	Kamble et al. (2018)

Reaction conditions

The improvement of TiO_2 properties by modification as mesoporous materials and introduction of metal as doping has been proven to help in enhancing the photocatalytic performance of the photocatalysts. These approaches are able to help decrease the wide E_g, extending the light absorption, produce high surface area and tunable pore diameter and exhibit more uniform morphologies [47, 68]. In this section, the utilization of modified TiO_2-based photocatalyst with mesoporous materials and metal doping for the elimination of organic pollutants will be discussed in detail. A summary of reaction conditions for photodegradation of organic pollutants using modified TiO_2-based photocatalysts is shown in Table 3.

Table 3. **Summary of reaction conditions for photodegradation of organic pollutants**

Photocatalyst	Synthesis method	Light source	Pollutant		Photocatalytic performance	References
			mg/L	mM		
I/TiO_2-T	Facile hydrolysis	Visible light	[p-CP]: 50	-	100% in 60 min	Chen et al. (2019)
Zr/mTiO_2	Dip-coating	Visible light	-	chloridazon: 0.005 phenol: 0.001 4-CP: 0.001	99% in 240 min	Mbiri et al. (2019)
Er/mTiO_2 NSPs	Solvothermal	Visible light	[RhB]: 10	-	98.78% in 28 min	Singh et al. (2018)
V/mTiO_2	Inverse micelle templated sol-gel	Visible light	[MB]: 32	-	100% in 120 min	Luo et al. (2015)

[2] described the synthesize of iodine (I)-doped mesoporous TiO_2 with lignin as a template (I/TiO_2-T) via facile hydrolysis method as the photocatalyst for photodegradation of p-chlorophenol (p-CP) with the irradiation of artificial visible light. The resultant photocatalyst revealed highest catalytic activity with the presence of lignin template and suitable amount of I-doping in which the complete degradation rate of p-CP was obtained within 60 min by using I-TiO_2-T catalyst compared to I-doped TiO_2 without lignin template (I/TiO_2), TiO_2 without I-doping (TiO_2-T) and P25 catalysts in which the results obtained for degradation of p-CP was 95.7, 10.7 and 5.5%, respectively, within 140 min under visible light absorption. The excellent result of I-TiO_2-T photocatalyst was because of the small grain size and large surface area of the catalyst. The I-doped TiO_2 promoted the I^{5+}-to-Ti^{4+} and the iodine-to-oxygen donor defects that might be triggered by visible light irradiation and hence, helped to achieve efficient pollutants degradation. Besides, the I-doping was able to further improve the photocatalytic performance by adjusting the E_g and the electrical properties of TiO_2.

[69] synthesized zirconium (Zr) doped mesoporous TiO_2 multilayer thin films (Zr/mTiO_2) by dip-coating. The catalyst was used for the removal of variety organic pollutants which were chloridazon, phenol and 4-CP through photodegradation under visible light irradiation. As the findings revealed, the Zr doped TiO_2 thin films with a Zr/Ti ratio of 0.05 exhibited better photocatalytic activity than pure TiO_2 thin films in which the photodegradation of chloridazon, phenol and 4-CP were degraded almost completely within 240 min of illumination but much lower activities was obtained by pure TiO_2 films for all these pollutants. The excellent performance was because of the huge surface area, better charge separation and stable anatase phase contributed by the incorporation of Zr

in Ti lattice positions as confirmed by BET, PL and X-ray diffraction (XRD) characterization results, respectively.

Previous study reported by [8] synthesized Erbium (Er) doped mesoporous TiO_2 nanospheres (Er/mTiO_2 NSPs) photocatalyst via solvothermal method for the degradation of Rhodamine B (RhB) as a pollutant. The excellent photocatalytic activity showed by the samples with 1mM of Er (TiO_2@Er1) in which 98.78% of RhB removal was achieved within 28 min compared to pure TiO_2 which only degraded 84.27% of RhB after 60 min under visible light irradiation. The excellent results of TiO_2@Er1 photocatalyst was because of the incorporation of Erbium on the surface of mesoporous spheres which enhanced the O_2 adsorption and also the ability of mesoporous TiO_2 that provided large surface area which in turn improved the photocatalytic performance. Besides, TiO_2@Er1 photocatalyst also exhibited excellent photostability and can be recycled for next photocatalytic experiment as the structural integrity was maintained even it was used for previous photocatalytic reactions.

[70] reported that the photocatalytic activity was improved under visible light irradiation when the synthesized mesoporous TiO_2 containing anatase/rutile mixed phase. The results from this study revealed mesoporous TiO_2 with 61% anatase and 39% rutile composition had shown better photocatalytic activity than Degussa P25 in which the MB can be entirely degraded by the photocatalyst in 120 min under visible light irradiation. Meanwhile, only 28% of MB was removed by using commercial P25 with the same reaction pathways. The excellent result of mesoporous TiO_2 mixed phase is because of the synergetic effect between anatase and rutile that form staggered E_g when these two phases are combined and it also promotes high separation of charge carriers to occur across the phase junctions in which electrons move from rutile to anatase and holes move in the opposite direction which then both charges will further be transferred to surface sites. Besides, the introduction of vanadium (V) dopant in the photocatalyst also enhances the photocatalytic activity as it promotes the V^{4+}/V^{5+} pair that forms an impurity energy band around 2.1 eV, acting like an electron/hole trap reducing the recombination rate. Figure 12 illustrates the photocatalytic mechanism of mesoporous anatase/rutile mixed phase TiO_2 materials with introduction of vanadium dopant (V/mTiO_2).

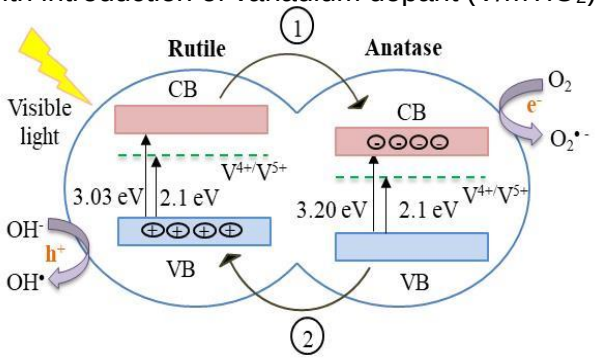

Figure 12. Schematic illustration of photocatalytic mechanism of V/mTiO_2.

CONCLUSION AND FUTURE PROSPECTS

In this review, the modification of TiO_2-based photocatalysts has been described by introducing the mesoporous materials and metal doping into TiO_2 for enhancing the photocatalytic activity in degrading various pollutants in wastewater and thus, provides the right direction into the strategy to obtain efficient photocatalytic performance. Furthermore, the synergistic effect of various methods employed, special criteria of the metal dopants and support materials, and their impact to photocatalytic activity had an extensive discussion.

Various utilization of synthesis methods and materials of TiO_2-based photocatalyst helped in better control of morphology and improve the reaction activity. On the other hand, the use of mesoporous materials has gained attention since they promote high surface area, various morphologies and compositions besides possessing uniform and tunable pore sizes resulting in high density of reactive sites and efficient mass transport. Then, doping TiO_2 with metal elements does not only reduce the E_g by adoption of ions that generate to be donors or acceptors, but also minimizes the recombination of electron-hole pairs. The introduction of these ions in nanostructured TiO_2 has enhanced its photocatalytic properties and extending to visible-light picking ability.

This review is hoped to provide the useful information for us to synthesize modified TiO_2-based photocatalysts with plenty active sites, long-life electron-hole pairs and tremendous light harvesting that may offer efficient photodegradation activity. Other than the success of tremendous photocatalytic performance by modification of TiO_2-based photocatalysts, further efforts are needed to improve the efficiency and reusability of these nanomaterials for profitable use. For an example, using the visible light-responsive photocatalysts is still at the undeveloped stage and more improvements are needed to reduce the high cost, technical hurdles, and possible environmental and human risks. Therefore, a suggestion for future study has to focus on the design of an effective photoreactor for the full utilization of solar energy to decrease the electricity costs. The build-up of suitable photoreactors can help in better harvest solar energy, accommodate the photocatalysts and reactants and also collect the reaction products in which can encourage the application of photocatalytic processes at an industrial level with efficient results.

ACKNOWLEDGEMENTS

This study was supported by a grant from Ministry of Higher Education through Fundamental Research Grant Scheme for Research Acculturation of Early Career Researchers (FRGS-RACER, no. 2019-0164-103-62).

REFERENCES

1. Sescu, A.M., et al., *TiO_2 doped with noble metals as an efficient solution for the photodegradation of hazardous organic water pollutants at ambient conditions.* Water, 2021. **13**(1): p. 19.DOI: https://doi.org/10.3390/w13010019.
2. Chen, W., et al., *Non-noble metal Co as active sites on TiO_2 nanorod for promoting photocatalytic H_2 production.* Materials Research Bulletin, 2019. **116**: p. 16-21.DOI: https://doi.org/10.1016/j.materresbull.2019.04.011.
3. Altın, İ., M. Sökmen, and Z. Bıyıklıoğlu, *Sol gel synthesis of cobalt doped TiO_2 and its dye sensitization for efficient pollutant removal.* Materials Science in Semiconductor Processing, 2016. **45**: p. 36-44.DOI: https://doi.org/10.1016/j.mssp.2016.01.016.

4. Blanco-Vega, M.P., et al., *Photocatalytic elimination of bisphenol A under visible light using Ni-doped TiO_2 synthesized by microwave assisted sol-gel method.* Materials Science in Semiconductor Processing, 2017. **71**: p. 275-282.DOI: https://doi.org/10.1016/j.mssp.2017.08.013.
5. Radtke, A., et al., *The structure and the photocatalytic activity of titania based nanotube and nanofiber coatings.* Applied Surface Science, 2016. **368**: p. 165-172.DOI: https://doi.org/10.1016/j.apsusc.2016.01.219.
6. Sood, S., et al., *Highly effective Fe-doped TiO_2 nanoparticles photocatalysts for visible-light driven photocatalytic degradation of toxic organic compounds.* Journal of colloid and interface science, 2015. **450**: p. 213-223.DOI: https://doi.org/10.1016/j.jcis.2015.03.018.
7. Islam, M.T., et al., *Development of photocatalytic paint based on TiO_2 and photopolymer resin for the degradation of organic pollutants in water.* Science of the Total Environment, 2020. **704**: p. 135406.DOI: https://doi.org/10.1016/j.scitotenv.2019.135406.
8. Singh, K., et al., *Erbium doped TiO_2 interconnected mesoporous spheres as an efficient visible light catalyst for photocatalytic applications.* Applied Surface Science, 2018. **449**: p. 755-763.DOI: https://doi.org/10.1016/j.apsusc.2018.01.279.
9. He, X., et al., *Photocatalytic degradation of microcystin-LR by modified TiO_2 photocatalysis: A review.* Science of The Total Environment, 2020. **743**: p. 140694.DOI: https://doi.org/10.1016/j.scitotenv.2020.140694.
10. Razali, N.A. and S.A. Othman, *Study of photocatalytic performance of doping titanium dioxide (TiO_2).* Journal of Science and Mathematics Letters, 2021. **9**: p. 72-79.
11. Singh, T., et al., *Application of TiO_2 nanoparticle in photocatalytic degradation of organic pollutants*. Materials Science Forum, 2016. **855**: p. 20-32.DOI: https://doi.org/10.4028/www.scientific.net/MSF.855.20.
12. Sonu., et al., *Review on augmentation in photocatalytic activity of $CoFe_2O_4$ via heterojunction formation for photocatalysis of organic pollutants in water.* Journal of Saudi Chemical Society, 2019. **23**: p. 1119-1136.
13. Bhanvase, B.A., T.P. Shende, and S.H. Sonawane, *A review on graphene–TiO_2 and doped graphene–TiO_2 nanocomposite photocatalyst for water and wastewater treatment.* Environmental Technology Reviews, 2017. **6**(1): p. 1-14.DOI: https://doi.org/10.1080/21622515.2016.1264489.
14. Chanu, L.A., et al., *Effect of operational parameters on the photocatalytic degradation of Methylene blue dye solution using manganese doped ZnO nanoparticles.* Results in Physics, 2019. **12**: p. 1230-1237.DOI: https://doi.org/10.1016/j.rinp.2018.12.089.
15. Pham, X.N., et al., *Synthesis of Ag-AgBr/Al-MCM-41 nanocomposite and its application in photocatalytic oxidative desulfurization of dibenzothiophene.* Advanced Powder Technology, 2018. **29**(8): p. 1827-1837.DOI: https://doi.org/10.1016/j.apt.2018.04.019.
16. Sun, H., et al., *High photodegradation ability of dyes by Fe (III)-tartrate/TiO_2 nanotubular photocatalyst supported via photo-Fenton reaction.* Journal of Photochemistry and Photobiology A: Chemistry, 2017. **334**: p. 20-25.DOI: https://doi.org/10.1016/j.jphotochem.2016.10.033.
17. Saravanan, R., et al., *ZnO/Ag/CdO nanocomposite for visible light-induced photocatalytic degradation of industrial textile effluents.* Journal of colloid and interface science, 2015. **452**: p. 126-133.DOI: https://doi.org/10.1016/j.jcis.2015.04.035.
18. Subramaniam, M.N., et al., *Adsorption and photocatalytic degradation of methylene blue using high surface area titanate nanotubes (TNT) synthesized via hydrothermal method.* Journal of Nanoparticle Research, 2017. **19**(6): p. 1-13.DOI: https://doi.org/10.1007/s11051-017-3920-9.
19. Geng, Y., et al., *Synthesis of Co doped BiVO4 with enhanced visible-light photocatalytic activities.* Journal of Alloys and Compounds, 2015. **651**: p. 744-748.DOI: https://doi.org/10.1016/j.jallcom.2015.08.123.
20. Anjugam Vandarkuzhali, S.A., et al., *Ultrasmall plasmonic nanoparticles decorated hierarchical mesoporous TiO_2 as an efficient photocatalyst for photocatalytic degradation of textile dyes.* ACS omega, 2018. **3**(8): p. 9834-9845.DOI: https://doi.org/10.1021/acsomega.8b01322.
21. Atchudan, R., et al., *In-situ green synthesis of nitrogen-doped carbon dots for bioimaging and TiO_2 nanoparticles@ nitrogen-doped carbon composite for photocatalytic degradation of organic pollutants.* Journal of Alloys and Compounds, 2018. **766**: p. 12-24.DOI: https://doi.org/10.1016/j.jallcom.2018.06.272.
22. Reddy, P.A.K., et al., *Recent advances in photocatalytic treatment of pollutants in aqueous media.* Environment international, 2016. **91**: p. 94-103.DOI: https://doi.org/10.1016/j.envint.2016.02.012.

23. Malika, M. and S.S. Sonawane, *Statistical modelling for the Ultrasonic photodegradation of Rhodamine B dye using aqueous based Bi-metal doped TiO_2 supported montmorillonite hybrid nanofluid via RSM.* Sustainable Energy Technologies and Assessments, 2021. **44**: p. 100980.DOI: https://doi.org/10.1016/j.seta.2020.100980.
24. Siddiqa, A., et al., *Cobalt and sulfur co-doped nano-size TiO_2 for photodegradation of various dyes and phenol.* Journal of Environmental Sciences, 2015. **37**: p. 100-109.DOI: https://doi.org/10.1016/j.jes.2015.04.024.
25. Abdennouri, M., et al., *Photocatalytic degradation of pesticides by titanium dioxide and titanium pillared purified clays.* Arabian Journal of Chemistry, 2016. **9**: p. S313-S318.DOI: https://doi.org/10.1016/j.arabjc.2011.04.005.
26. Radtke, A., *The structure and the photocatalytic activity of titania based nanotube and nanofiber coatings.* Applied Surface Science, 2016. **368**: p. 165-172.DOI: https://doi.org/10.1016/j.clay.2017.02.029.
27. Szczepanik, B., *Photocatalytic degradation of organic contaminants over clay-TiO_2 nanocomposites: A review.* Applied Clay Science, 2017. **141**: p. 227-239.DOI: https://doi.org/10.1016/j.clay.2017.02.029.
28. Azami, M.S., et al., *Formation of an amorphous carbon nitride/titania composite for photocatalytic degradation of RR4 dye.* Journal of Water Process Engineering, 2020. **35**: p. 101209.DOI: https://doi.org/10.1016/j.jwpe.2020.101209.
29. Hitam, C.N.C., et al., *Effect of carbon-interaction on structure-photoactivity of Cu doped amorphous TiO_2 catalysts for visible-light-oriented oxidative desulphurization of dibenzothiophene.* Fuel, 2018. **216**: p. 407-417.DOI: https://doi.org/10.1016/j.fuel.2017.12.035.
30. Mohamed, M.A., et al., *Carbon as amorphous shell and interstitial dopant in mesoporous rutile TiO_2: Bio-template assisted sol-gel synthesis and photocatalytic activity.* Applied Surface Science, 2017. **393**: p. 46-59.DOI: https://doi.org/10.1016/j.apsusc.2016.09.145.
31. Parangi, T. and M.K. Mishra, *Titania nanoparticles as modified photocatalysts: a review on design and development.* Comments on Inorganic Chemistry, 2019. **39**(2): p. 90-126.DOI: https://doi.org/10.1080/02603594.2019.1592751.
32. Anandan, S., T. Sivasankar, and T. Lana-Villarreal, *Synthesis of TiO_2/WO_3 nanoparticles via sonochemical approach for the photocatalytic degradation of methylene blue under visible light illumination.* Ultrasonics sonochemistry, 2014. **21**(6): p. 1964-1968.DOI: https://doi.org/10.1016/j.ultsonch.2014.02.015.
33. Al-Mamun, M.R., et al., *Photocatalytic activity improvement and application of UV-TiO_2 photocatalysis in textile wastewater treatment: A review.* Journal of Environmental Chemical Engineering, 2019. **7**(5): p. 103248.DOI: https://doi.org/10.1016/j.jece.2019.103248.
34. Zhu, D. and Q. Zhou, *Action and mechanism of semiconductor photocatalysis on degradation of organic pollutants in water treatment: A review.* Environmental Nanotechnology, Monitoring & Management, 2019. **12**: p. 100255.DOI: https://doi.org/10.1016/j.enmm.2019.100255.
35. Teh, C.Y., T.Y. Wu, and J.C. Juan, *An application of ultrasound technology in synthesis of titania-based photocatalyst for degrading pollutant.* Chemical Engineering Journal, 2017. **317**: p. 586-612.DOI: https://doi.org/10.1016/j.cej.2017.01.001.
36. Kumar, A. and G. Pandey, *Different methods used for the synthesis of TiO_2 based nanomaterials: A review.* Am. J. Nano Res. Appl, 2018. **6**(1): p. 1-10.DOI: https://doi.org/10.11648/j.nano.20180601.11.
37. Nasr, M., et al., *Recent progress on titanium dioxide nanomaterials for photocatalytic applications.* ChemSusChem, 2018. **11**(18): p. 3023-3047.DOI: https://doi.org/10.1002/cssc.201800874.
38. Nasr, M., et al., *Enhanced photocatalytic performance of novel electrospun BN/TiO_2 composite nanofibers.* New Journal of Chemistry, 2017. **41**(1): p. 81-89.DOI: https://doi.org/10.1039/C6NJ03088B.
39. Arfanis, M.K., et al., *Photocatalytic degradation of salicylic acid and caffeine emerging contaminants using titania nanotubes.* Chemical Engineering Journal, 2017. **310**: p. 525-536.DOI: https://doi.org/10.1016/j.cej.2016.06.098.
40. Arfanis, M.K., et al., *Photocatalytic properties of copper—Modified core-shell titania Nanocomposites.* Journal of Photochemistry and Photobiology A: Chemistry, 2019. **370**: p. 145-155.DOI: https://doi.org/10.1016/j.jphotochem.2018.10.051.
41. Ovodok, E., et al., *Synthesis and characterization of efficient TiO_2 mesoporous photocatalysts.* Materials Today: proceedings, 2017. **4**(11): p. 11526-11533.DOI: https://doi.org/10.1016/j.matpr.2017.09.062.

42. Zhang, Y., et al., *Non-uniform doping outperforms uniform doping for enhancing the photocatalytic efficiency of Au-doped TiO_2 nanotubes in organic dye degradation.* Ceramics International, 2017. **43**(12): p. 9053-9059.DOI: https://doi.org/10.1016/j.ceramint.2017.04.050.
43. Zhang, W., et al., *Recent advances in the synthesis of hierarchically mesoporous TiO_2 materials for energy and environmental applications.* National Science Review, 2020. **7**(11): p. 1702-1725.DOI: https://doi.org/10.1093/nsr/nwaa021.
44. Niu, B., et al., *Mesoporous titanium dioxide: Synthesis and applications in photocatalysis, energy and biology*. Materials, 2018. **11**(10): p. 1910.DOI: https://doi.org/10.3390/ma11101910.
45. Bagheri, S., et al., *Progress on mesoporous titanium dioxide: synthesis, modification and applications.* Microporous and Mesoporous Materials, 2015. **218**: p. 206-222.DOI: https://doi.org/10.1016/j.micromeso.2015.05.028.
46. Chowdhury, I.H. and M.K. Naskar, *Sol-gel synthesis of mesoporous hollow titania microspheres for photodegradation of 4-chlorophenol.* Indian Journal Of Chemistry Section A-Inorganic Bio-Inorganic Physical Theoretical & Analytical Chemistry, 2018. **57**(7): p. 910-914.DOI: https://doi.org/10.1016/j.ceramint.2015.10.049.
47. Jaafar, N.F., et al., *New insights into self-modification of mesoporous titania nanoparticles for enhanced photoactivity: Effect of microwave power density on formation of oxygen vacancies and Ti^{3+} defects.* RSC advances, 2015. **5**(110): p. 90991-91000.DOI: https://doi.org/10.1039/C5RA15120A.
48. Khalid, N.R., et al., *Carbonaceous-TiO_2 nanomaterials for photocatalytic degradation of pollutants: A review.* Ceramics International, 2017. **43**(17): p. 14552-14571.DOI: https://doi.org/10.1016/j.ceramint.2017.08.143.
49. Zhiming, S., et al., *Effects of Pre-annealing Atmosphere on Microstructure and Photocatalytic Activities of Fe-doped Titania Nanotubes.* Rare Metal Materials and Engineering, 2017. **46**(11): p. 3244-3252.DOI: https://doi.org/10.1016/S1875-5372(18)30037-7.
50. Yu, J. H., et al., *Oxidation state and structural studies of vanadium-doped titania particles for the visible light-driven photocatalytic activity.* Applied Surface Science, 2018. **472**: p. 46-53.DOI: https://doi.org/10.1016/j.apsusc.2018.04.125.
51. Camarillo, R., et al., *Enhancing the photocatalytic reduction of CO_2 with undoped and Cu-doped TiO_2 nanofibers synthesized in supercritical medium.* The Journal of Supercritical Fluids, 2019. **147**: p. 70-80.DOI: https://doi.org/10.1016/j.supflu.2019.02.013.
52. Mohseni-Salehi, M.S., E. Taheri-Nassaj, and M. Hosseini-Zori, *Effect of dopant (Co, Ni) concentration and hydroxyapatite compositing on photocatalytic activity of titania towards dye degradation.* Journal of Photochemistry and Photobiology A: Chemistry, 2018. **356**: p. 57-70.DOI: https://doi.org/10.1016/j.jphotochem.2017.12.027.
53. Samet, L., et al., *Effect of gamma radiation on the photocatalytic properties of Cu doped titania nanoparticles.* Materials Research Bulletin, 2018. **107**: p. 1-7.
54. Humayun, M., et al., *Modification strategies of TiO_2 for potential applications in photocatalysis: a critical review.* Green Chemistry Letters and Reviews, 2018. **11**(2): p. 86-102.DOI: https://doi.org/10.1080/17518253.2018.1440324.
55. Fang, W., M. Xing, and J. Zhang, *Modifications on reduced titanium dioxide photocatalysts: A review.* Journal of Photochemistry and Photobiology C: Photochemistry Reviews, 2017. **32**: p. 21-39.DOI: https://doi.org/10.1016/j.jphotochemrev.2017.05.003.
56. Ribao, P., et al., *Role of reactive oxygen species on the activity of noble metal-doped TiO_2 photocatalysts.* Journal of hazardous materials, 2019. **372**: p. 45-51.DOI: https://doi.org/10.1016/j.jhazmat.2018.05.026.
57. Zhang, F., et al., *A novel preparation of Ag-doped TiO_2 nanofibers with enhanced stability of photocatalytic activity.* RSC Advances, 2015. **5**(41): p. 32088-32091.DOI: https://doi.org/10.1039/C5RA01353D.
58. Ali, T., et al., *Enhanced photocatalytic and antibacterial activities of Ag-doped TiO_2 nanoparticles under visible light.* Materials Chemistry and Physics, 2018. **212**: p. 325-335.DOI: https://doi.org/10.1016/j.matchemphys.2018.03.052.
59. Lakshmanareddy, N., et al., *Pt/TiO_2 nanotube photocatalyst–Effect of synthesis methods on valance state of Pt and its influence on hydrogen production and dye degradation.* Journal of colloid and interface science, 2019. **538**: p. 83-98.DOI: https://doi.org/10.1016/j.jcis.2018.11.077.
60. Khaki, M.R.D., et al., *Application of doped photocatalysts for organic pollutant degradation-A review.* Journal of environmental management, 2017. **198**: p. 78-94.DOI: https://doi.org/10.1016/j.jenvman.2017.04.099.

61. Shayegan, Z., C. S. Lee, and F. Haghighat, *TiO_2 photocatalyst for removal of volatile organic compounds in gas phase–A review.* Chemical Engineering Journal, 2018. **334**: p. 2408-2439.DOI: https://doi.org/10.1016/j.cej.2017.09.153.
62. Shafei, A. and S. Sheibani, *Visible light photocatalytic activity of Cu doped TiO_2-CNT nanocomposite powder prepared by sol–gel method.* Materials Research Bulletin, 2019. **110**: p. 198-206.DOI: https://doi.org/10.1016/j.materresbull.2018.10.035.
63. Biru, M., et al., *Preparation and Characterization of Copper, Iron, and Nickel Doped Titanium Dioxide Photocatalysts for Decolorization of Methylene Blue.* Sains Malaysiana, 2021. **50**(1): p. 135-149.DOI: https://doi.org/10.17576/jsm-2021-5001-14.
64. Ong, C.B., L.Y. Ng, and A.W. Mohammad, *A review of ZnO nanoparticles as solar photocatalysts: Synthesis, mechanisms and applications.* Renewable and Sustainable Energy Reviews, 2018. **81**: p. 536-551.DOI: https://doi.org/10.1016/j.rser.2017.08.020.
65. Rodríguez, P.A.O., et al., *A simple synthesis way to obtain iron-doped TiO_2 nanoparticles as photocatalytic surfaces.* Chemical Physics Letters, 2019. **732**: p. 136643.DOI: https://doi.org/10.1016/j.cplett.2019.136643.
66. Nasirian, M., et al., *Enhancement of photocatalytic activity of titanium dioxide using non-metal doping methods under visible light: a review.* International Journal of Environmental Science and Technology, 2018. **15**(9): p. 2009-2032.DOI: https://doi.org/10.1007/s13762-017-1618-2.
67. Kamble, R., et al., *Visible light-driven high photocatalytic activity of Cu-doped TiO_2 nanoparticles synthesized by hydrothermal method.* Material Science Research India, 2018. **15**(3): p. 197-208.DOI: https://doi.org/10.13005/msri/150301.
68. Basavarajappa, P.S., et al., *Recent progress in metal-doped TiO_2, non-metal doped/codoped TiO_2 and TiO_2 nanostructured hybrids for enhanced photocatalysis.* International Journal of Hydrogen Energy, 2020. **45**(13): p. 7764-7778.DOI: https://doi.org/10.1016/j.ijhydene.2019.07.241.
69. Mbiri, A., et al., *Zirconium doped mesoporous TiO_2 multilayer thin films: Influence of the zirconium content on the photodegradation of organic pollutants.* Catalysis Today, 2019. **328**: p. 71-78.DOI: https://doi.org/10.1016/j.cattod.2019.01.043.
70. Luo, Z., et al., *Crystalline mixed phase (anatase/rutile) mesoporous titanium dioxides for visible light photocatalytic activity*. Chemistry of Materials, 2015. **27**(1): p. 6-17.DOI: https://doi.org/10.1021/cm5035112.
71. Petronella, F., et al., *Scalable Synthesis of Mesoporous TiO_2 for Environmental Photocatalytic Applications.* Materials, 2019. **12**(11): p. 1-21.DOI: https://doi.org/10.3390/ma12111853.
72. Chowdhury, I.H., S. Ghosh, and M.K. Naskar, *Aqueous-based synthesis of mesoporous TiO_2 and Ag–TiO_2 nanopowders for efficient photodegradation of methylene blue.* Ceramics International, 2016. **42**(2): p. 2488-2496.DOI: https://doi.org/10.1016/j.ceramint.2015.10.049.
73. Byranvand, M. M., et al., *A Review on Synthesis of Nano-TiO_2 via Different Methods*. Journal of Nanostructures, 2013. **3**(1): p. 1-9.DOI: https://doi.org/10.7508/JNS.2013.01.001.
74. Chen, D., et al., *Photocatalytic degradation of organic pollutants using TiO_2-based photocatalysts: A review.* Journal of Cleaner Production, 2020. p. 1-14.DOI: https://doi.org/10.1016/j.jclepro.2020.121725
75. Fernandes, A., et al., *Integrated photocatalytic advanced oxidation system (TiO_2/UV/O_3/H_2O_2) for degradation of volatile organic compounds*. Separation and Purification Technology, 2019. **224**: p. 1-14.DOI: https://doi.org/10.1016/j.seppur.2019.05.012
76. Reddy, P.V.L., et al., *TiO_2-based photocatalytic disinfection of microbes in aqueous media: A review* . Environmental Research, 2017. **154**: p. 296-303.DOI: https://doi.org/10.1016/j.envres.2017.01.018.